PERFORMANCE ANALYSIS AND OPTIMIZATION OF RECTANGULAR FIN ARRAYS USED IN PLATE-FIN HEAT EXCHANGERS

by

Weicheng WU and Hassan SOLIMAN*

Department of Mechanical Engineering, University of Manitoba, Winnipeg, Canada

Original scientific paper
https://doi.org/10.2298/TSCI190926213W

This paper deals with longitudinal rectangular fin arrays used in plate-fin heat exchangers. The temperature distribution and rate of heat transfer were obtained using 1-D and 2-D solutions. The ranges of independent parameters within which the 1-D solution was within 1% from the 2-D solution were determined. Simple analytical solutions were determined for the rate of heat transfer, fin effectiveness, and augmentation factor. The aspect ratio at which the rate of heat transfer reached a maximum was determined, as well as the corresponding effectiveness and augmentation factor.

Key words: *plate-fin module, longitudinal rectangular fins, heat transfer, fin effectiveness, augmentation factor, optimum values*

Introduction

Most energy conversion systems include heat exchangers as essential parts. There are several examples in industry, *e.g.*, cooling of electronic packages, heat recovery systems, heating and cooling systems, transport, and power-generating systems. One of the most commonly used heat exchanger modules is the plate-fin channels. Optimizing the performance of these channels would obviously lead to material saving and/or lower energy consumption. The focus in this study will be on optimizing the fin performance for maximum rate of heat transfer.

The size of the literature on the performance analysis and optimization of fins is immense. It includes fins with various geometries, cross-sections, boundary conditions, constant and variable area, constant and variable properties, with and without heat generation, and different modes of heat dissipation. This study deals with longitudinal fins with uniform rectangular cross-sections.

For single detached fins, reviews of several research efforts on the performance and optimization of fins can be found in Kern and Kraus [1], Kraus *et al.* [2], Razelos [3], and Nagarani *et al.* [4]. The optimization analyses in these works considered primarily the boundary conditions of adiabatic tip and convective tip. The case of fins with a prescribed tip temperature was investigated by Soliman and Elazhary [5] and Marchildon and Soliman [6]. The vast majority of the work in [1-6] employed 1-D analysis.

More recently, the case of fin arrays attached at the base to a wall was considered. Alarcon *et al.* [7] studied the optimization of a longitudinal rectangular fin-wall assembly with a fixed volume using a 1-D analysis. Restrictions were introduced, such as a fixed fin pitch, wall thickness greater than fin thickness, and fin aspect ratio limited to a specific range. Kuo *et al.*

* Corresponding author, e-mail: hassan.soliman@umanitoba.ca

[8] considered the geometry of a longitudinal fin assembly attached to a plate (simulating a heat sink). The fin cross-section was either square, rectangular, equilateral triangle, or cylindrical. The number of fins and the volume of each fin were fixed, and the objective of the study was to find the optimal length and cross-sectional area of the fins that produced maximum heat transfer rate from the fins and plate combined for each cross-sectional shape. Franco [9] used a similar geometry as the one used in [8] with simple convection applied on the unfinned surface and 1-D heat transfer in the fins. The input parameters to the optimization problem were: the height and width of the base surface, the interfin spacing, the base temperature, the fluid temperature, and the total volume of the base and fins. With these input data, an algorithm was used to determine the number of fins, the fin thickness and the fin height that produces maximum heat dissipation. Kundu and Das [10] considered fin arrays attached to a plate with four geometries (longitudinal rectangular, annular rectangular, longitudinal trapezoidal, and annular trapezoidal). They employed 1-D analysis and reported results for fin efficiency and fin effectiveness. In their optimization problem, the total volume and the total height of the assembly, the interfin spacing and the wall thickness were assumed constant, and the optimum fin dimensions for maximum heat transfer were determined. Kang [11] considered the case of a single pin fin attached to a base with variable thickness. The optimum heat loss, the corresponding optimum fin effectiveness, fin length, and fin diameter were presented as functions of the base thickness and fin volume. It was found that the optimum heat loss, the corresponding optimum fin effectiveness, and the optimum fin length decrease with an increase in the fin base thickness. Also, an increase in the fin volume resulted in an increase in the optimum heat loss, but a decrease in the corresponding optimum effectiveness. Lin and Chen [12] reported 1-D analysis of vertical plate fins attached to an isothermal base with adiabatic fin tips. Different heat transfer coefficients were assumed on the base surface and the fin surface. For fixed fin length, fin thickness, and total base height, they solved for the fin spacing that gives maximum heat dissipation. Luna-Abad *et al.* [13] considered fin-wall assemblies with longitudinal rectangular fins and constant temperature on the unfinned side of the wall. The geometry was simplified by assuming fixed wall dimensions (height, width, and thickness). The input parameters for the design were the fin volume, ratio of convection coefficient to thermal conductivity, and ratio of convection coefficients on the fin and the wall between the fins. The relative-inverse-admittance procedure was used to optimize the fin thickness for maximum heat dissipation.

Although there has been a large volume of articles on the performance and optimization of single fins and fin-wall assemblies, very few studies were reported on the analysis of fins attached to two plates, as in plate-fin heat exchangers. Yang *et al.* [14] investigated a plate-fin module with offset strip fin and plain fin in laminar flow using a CFD (FLUENT) code. The cover plate had a fixed thickness of 1 mm. They noted that the offset strip fin performed better at low Reynolds numbers, while the plain fin was better at higher Reynolds numbers. Wen *et al.* [15] used the same fin geometries in [14] and the same flow condition (laminar). The main focus was on the optimization method and they concluded that using a combined Kriging response surface and multi-objective genetic algorithm in optimizing the fin design was faster to converge and more cost effective than other existing methods.

The objective of the present study is to investigate the performance of a plate-fin module and to optimize the fin design for maximum rate of heat transfer. The focus here will be on developing simple solutions that are easy to use and hopefully provide some guidance for the design engineer.

Physical model and mathematical formulation

The geometry under consideration, consisting of two parallel plates with an array of rectangular fins attached to the plates, is shown in fig. 1(a). Due to symmetry, the computational domain reduces to the module shown in fig. 1(b). In this module, the plates have a height, H, and thickness, W. The half fin in the module has a length, L, and a thickness, t. It is assumed that the geometry is 2-D, *i.e.*, the dimension normal to the x-y plane is much larger than all other dimensions. The outer surfaces of the plates are maintained at temperatures T_1 and T_2, and it is assumed that $T_1 \geq T_2$. The surfaces at $0 \leq x \leq (L + 2W)$ and $y = 0$, $0 \leq x \leq W$ and $y = H$, $(L + W) \leq x \leq (L + 2W)$ and $y = H$ are adiabatic due to symmetry. All the other (internal) surfaces are exposed to convection with a fluid at a temperature T_∞ where $T_\infty < T_2 \leq T_1$, and a heat transfer coefficient, h. The objective of this study is to determine the geometrical parameters that would result in maximum heat dissipation by the module (*i.e.*, maximum heat convection the fluid).

The present analysis was conducted under the following assumptions:

– Steady-state heat transfer with uniform thermal properties.
– The fin is made from the same material of the wall in order to decrease the number of independent variables.
– Constant heat transfer coefficient.

Two different formulations were applied using one- and 2-D approaches. A comparison was conducted between the two solutions in order to determine the range over which the 1-D solution is within 1% from the more accurate 2-D solution.

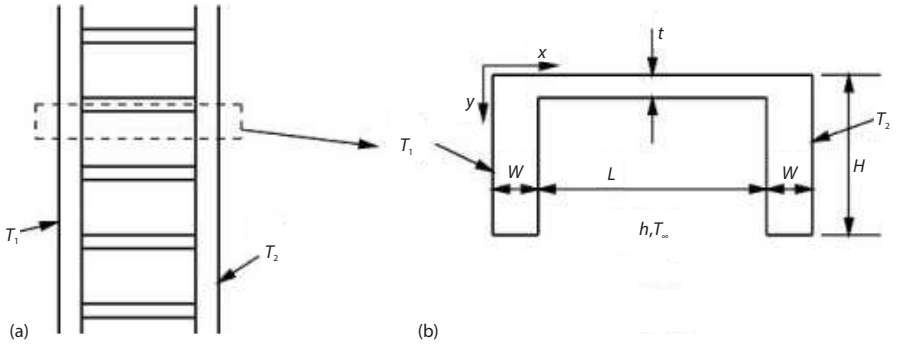

Figure 1. Geometry and co-ordinate system

The 2-D formulation

The applicable energy equation for heat conduction throughout the domain:

$$\frac{\partial^2 T}{\partial x^2} + \frac{\partial^2 T}{\partial y^2} = 0 \tag{1}$$

subject to the boundary conditions stated previously for all surfaces. The following dimensionless groups were introduced:

$$\alpha = \frac{t}{L},\ \beta = \frac{W}{L_c},\ \gamma = \frac{H}{L_c},\ \text{and}\ \ \text{Bi} = \frac{hL_c}{k} \tag{2}$$

where L_c is a characteristic length given by $L_c = (Lt)^{1/2}$. For a given value of h/k, we can determine the value of L_c from Bi, the value of H from γ, the value of W from β, and the values of L and t from α ($L = L_c/\alpha^{1/2}$ and $t = L_c\alpha^{1/2}$). Therefore, the geometry is completely defined by the

four independent parameters in eq. (2). Other parameters that will be used in the analysis are: the excess temperature, θ, is given:

$$\theta = T - T_\infty \tag{3a}$$

with the excess temperatures at the outer surfaces of the plates, $\theta_1 = T_1 - T_\infty$ and $\theta_2 = T_2 - T_\infty$, and the dimensionless rate of heat transfer, Q:

$$Q = \frac{q}{k\left(T_1 - T_\infty\right)} = \frac{q}{k\theta_1} \tag{3b}$$

With a known value of θ_2/θ_1, an arbitrary value of θ_1 can be assumed from which θ_2 can be obtained and the rate of heat transfer, q, can be calculated from the temperature profile obtained from the solution of eq. (1). This value of q would be proportional to θ_1 and therefore, Q in eq. (3b) is dependent only on θ_2/θ_1, but independent of θ_1. Thus, the geometry and the dimensionless rate of heat transfer are dependent on α, β, γ, Bi, and θ_2/θ_1.

Constraints were applied on the values of α, β, and γ in order to avoid unreasonable or impossible dimensions (such as negative values). First, the aspect ratio, α, was limited to the practical range $0.02 \leq \alpha \leq 0.2$. Next, the wall thickness was assumed to be at least equal to the fin thickness, *i.e.*, $W \geq 2t$ for rigidity. Finally, in order to ensure adequate inter-fin spacing for proper cooling, the constraint $H \geq 3t$ was imposed (*i.e.*, the inter-fin spacing is at least equal to a full fin thickness). These constraints result in the relations:

$$\beta = \frac{W}{L_c} = \frac{W}{\sqrt{Lt}} = \frac{W}{t}\sqrt{\alpha} \geq 2\sqrt{\alpha} \tag{4a}$$

and

$$\gamma = \frac{H}{L_c} = \frac{H}{\sqrt{Lt}} = \frac{H}{t}\sqrt{\alpha} \geq 3\sqrt{\alpha} \tag{5}$$

A numerical finite control volume method was used in generating the solutions. Each wall was divided into N_{x1} subdivisions in the x-direction and the fin was divided into N_{x2} subdivisions in the x-direction. The fin and the finned parts of the walls were divided into N_{y1} subdivisions in the y-direction and the un-finned parts of the walls were divided into N_{y2} subdivisions in the y-direction. The total number of control volumes in the computational domain is N.

Mesh independence tests were conducted to determine the appropriate values of N_{x1}, N_{x2}, N_{y1}, and N_{y2}. A sample of these results is shown in tab. 1. This sample corresponds to Bi = 0.01 and 1, α = 0.02 and 0.2, and θ_2/θ_1 = 0.5 and 1, while values of β and γ were set to β = 1 and γ = 4. These values insure that $\beta \geq 2(\alpha)^{1/2}$ and $\gamma \geq 3(\alpha)^{1/2}$.

It can be seen from tab. 1 that a mesh with 769 control volumes can produce results with at least three-significant-figures accuracy. More tests were conducted with other values of β and γ, and it was found that while β and γ have a significant influence on Q_{2D}, a mesh with 769 control volumes is still adequate for good accuracy.

The 1-D solution

An approximate solution based on 1-D conduction was formulated. The heat flow rates q_a, q_b, q_c, and q_d, shown in fig. 2, travel in the x-direction. Since the surfaces at $y = 0$ and $y = H$ are adiabatic, then the total rate of heat transfer into the fluid per unit depth, q_{1D}, will be the sum of these four heat rates, *i.e.*:

$$q_{1D} = q_a + q_b + q_c + q_d \tag{5}$$

Table 1. Sample of mesh-independence results

Bi	θ_2/θ_1	α	N_{x1}	N_{x2}	N_{y1}	N_{y2}	N	$Q_{2\text{-D}}$
0.01	1	0.02	6	6	6	6	157	0.129717
			12	15	6	12	487	0.128714
			15	30	6	15	769	0.128535
		0.2	6	6	6	6	157	0.092064
			12	15	6	12	487	0.092043
			15	30	6	15	769	0.092040
	0.5	0.02	6	6	6	6	157	0.097288
			12	15	6	12	487	0.096535
			15	30	6	15	769	0.096401
		0.2	6	6	6	6	157	0.069048
			12	15	6	12	487	0.069032
			15	30	6	15	769	0.069030
1	1	0.02	6	6	6	6	157	4.221645
			12	15	6	12	487	4.119038
			15	30	6	15	769	4.099523
			15	60	6	15	949	4.093916
		0.2	6	6	6	6	157	4.079226
			12	15	6	12	487	4.064639
			15	30	6	15	769	4.062496
	0.5	0.02	6	6	6	6	157	3.166234
			12	15	6	12	487	3.089278
			15	30	6	15	769	3.074642
			15	60	6	15	949	3.070437
		0.2	6	6	6	6	157	3.059419
			12	15	6	12	487	3.048479
			15	30	6	15	769	3.046872

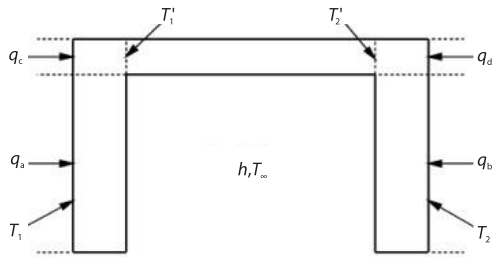

Figure 2. Schematic of the 1-D model

These four heat flow rates can be formulated:

$$q_{\mathrm{a}} = \frac{T_1 - T_\infty}{\dfrac{W}{k(H-t)} + \dfrac{1}{h(H-t)}} \tag{6a}$$

$$q_{\mathrm{b}} = \frac{T_2 - T_\infty}{\dfrac{W}{k(H-t)} + \dfrac{1}{h(H-t)}} \tag{6b}$$

$$q_{\mathrm{c}} = \frac{T_1 - T_1'}{\dfrac{W}{kt}} \tag{6c}$$

$$q_{\mathrm{d}} = \frac{T_2 - T_2'}{\dfrac{W}{kt}} \tag{6d}$$

These are four equations in six unknowns and two more relations are required. The temperature distribution in the half fin with prescribed temperatures T_1' and T_2' at the base and tip, respectively, is given [16]:

$$T - T_\infty = \frac{(T_2' - T_\infty)\sinh mx' + (T_1' - T_\infty)\sinh m(L - x')}{\sinh mL} \tag{7}$$

where $x' = x - W$ and $m = (h/kt)^{1/2}$. The two additional relations can be obtained by imposing continuity of heat flux in the fin at the base and the tip:

$$-kt\left(\frac{\mathrm{d}T}{\mathrm{d}x'}\right)_{x'=0} = q_{\mathrm{c}} \quad \text{and} \quad kt\left(\frac{\mathrm{d}T}{\mathrm{d}x'}\right)_{x'=L} = q_{\mathrm{d}} \tag{8}$$

Combining eqs. (6a) and (6b), and introducing the parameters defined in eqs. (2), (3a), and (3b) we get (after algebraic manipulation):

$$Q_{\mathrm{a}} + Q_{\mathrm{b}} = \frac{\left(1 + \dfrac{\theta_2}{\theta_1}\right)\left(\gamma - \sqrt{\alpha}\right)}{\beta + \dfrac{1}{\mathrm{Bi}}} \tag{9}$$

From eqs. (6c) and (6d), we get:

$$q_{\mathrm{c}} + q_{\mathrm{d}} = \frac{(\theta_1 + \theta_2) - (\theta_1' + \theta_2')}{\dfrac{W}{kt}} \tag{10a}$$

and combining eqs. (7) and (8) gives:

$$q_{\mathrm{c}} + q_{\mathrm{d}} = \frac{\sqrt{hkt}\,(\cosh mL - 1)(\theta_1' + \theta_2')}{\sinh mL} \tag{10b}$$

Equating (10a) and (10b), a formula for $(\theta_1' + \theta_2')$ was obtained and upon substituting in either eq. (10a) or eq. (10b), we get:

$$q_{\mathrm{c}} + q_{\mathrm{d}} = \frac{\sqrt{hkt}\,(\theta_1 + \theta_2)(\cosh mL - 1)}{\sqrt{hkt}\left[\dfrac{W}{kt}\right](\cosh mL - 1) + \sinh mL} \tag{11}$$

Equation (11) can be expressed in the dimensionless form:

$$Q_c + Q_d = \frac{\left(1+\frac{\theta_2}{\theta_1}\right)\sqrt{\alpha}}{\beta + \frac{\alpha^{1/4}\mathrm{Bi}^{-1/2}\sinh\left(\mathrm{Bi}^{1/2}\alpha^{-3/4}\right)}{\cosh\left(\mathrm{Bi}^{1/2}\alpha^{-3/4}\right)-1}} \tag{12}$$

Finally, the total rate of heat dissipation into the fluid per unit depth, $Q_{1\text{-D}}$, would be the sum of $(Q_a + Q_b)$ from eq. (9) and $(Q_c + Q_d)$ from eq. (12). It can be seen from this derivation that $Q_{1\text{-D}}$ is a function of α, β, γ, Bi, and θ_2/θ_1, similar to the 2-D case.

Results and discussion

Validity of the 1-D solution

The deviation between the 1- and 2-D results was found to increase as Bi and/or θ_2/θ_1 increase. Therefore, the comparison was carried out at the upper values of Bi = 1 and $\theta_2/\theta_1 = 1$. Results were generated for $0.02 \le \alpha \le 0.2$ and various values of β and γ, as shown in figs. 3 and 4. The deviation between the two solutions was defined:

$$E = \left|\frac{Q_{2\text{-D}} - Q_{1\text{-D}}}{Q_{2\text{-D}}}\right| \times 100\% \tag{13}$$

These figures show that for $\gamma = 3$, the deviation is less than 1% for a wide range of β and for $\beta = 1$, the deviation is less than 1% as long as $\gamma \ge 3$. Therefore, it is fair to conclude that reasonably accurate results can be generated from the 1-D solution as long as $\beta \ge 1$ and $\gamma \ge 3$. Substituting $\beta = 1$ and $\gamma = 3$ into eqs. (4a) and (4b) for the range $0.02 \le \alpha \le 0.2$, we get the following constraints on the plate thickness and the inter-fin spacing: $2.24 \le W/t \le 7.1$ and $6.7 \le H/t \le 21.3$.

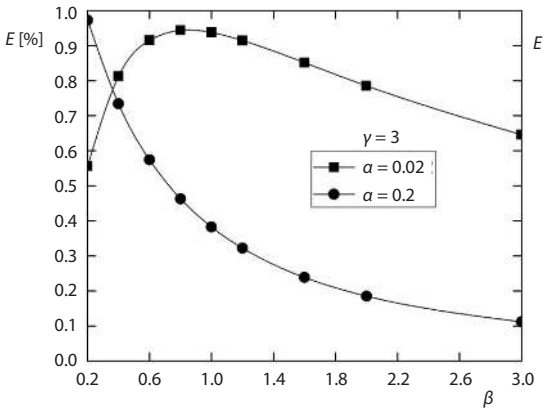

Figure 3. Deviation between 1-D and 2-D solutions at $\gamma = 3$ and various β

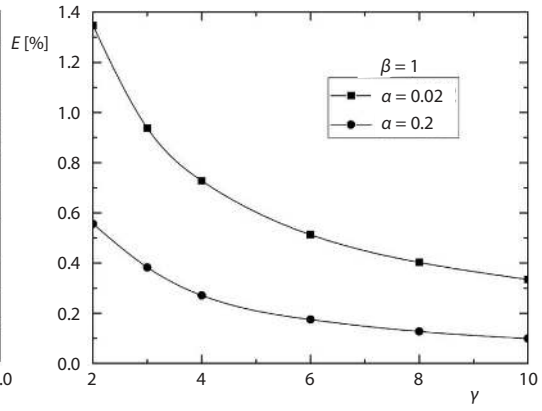

Figure 4. Deviation between 1-D and 2-D solutions at $\beta = 1$ and various γ

These constraints cover a wide range of practical applications, therefore, the 1-D solution will be used in generating the present results within the aforementioned constraints.

Fin effectiveness

The effectiveness is defined as the ratio of the rate of heat transfer dissipated by the fin to the rate of heat transfer through the contact areas between the fin and the two plates if the fin was not present. The dimensionless rate of heat transfer from the fin surface is equal to ($Q_c + Q_d$) given by eq. (12), while the rate of heat transfer from the contact areas between the fin and the two plates when the fin is not present:

$$q_w = \frac{(T_1 - T_\infty) + (T_2 - T_\infty)}{\frac{W}{kt} + \frac{1}{ht}} \tag{14}$$

Introducing the dimensionless parameters defined by eqs. (2), (3a), and (3b), we get:

$$Q_w = \frac{q_w}{k\theta_1} = \frac{\sqrt{\alpha}\left(1 + \frac{\theta_2}{\theta_1}\right)}{\beta + \frac{1}{\mathrm{Bi}}} \tag{15}$$

Therefore, the fin effectiveness can be expressed:

$$\varepsilon = \frac{Q_c + Q_d}{Q_w} = \frac{\beta + \frac{1}{\mathrm{Bi}}}{\beta + \frac{\alpha^{1/4}\mathrm{Bi}^{-1/2}\sinh\left(\mathrm{Bi}^{1/2}\alpha^{-3/4}\right)}{\cosh\left(\mathrm{Bi}^{1/2}\alpha^{-3/4}\right) - 1}} \tag{16}$$

Equation (16) shows that ε is a function of α, β, and Bi, but independent of γ and θ_2/θ_1. Figure 5 shows results for ε as a function of α at Bi = 0.05 and various values of β. It can be seen that ε decreases with an increase in α or β. The decrease in ε as the aspect ratio increases is consistent with the behaviour of single detached fins and also consistent with the results of Kundu and Das [10]. As well, an increase in β at the same Bi corresponds to an increase in wall thickness and the trend of decreasing ε with increasing β is consistent with Kang [11]. On the other hand, if β goes to zero, the fin becomes a detached fin with temperature T_1 at the base and T_2 at the tip. For this limiting case, eq. (16) reduces to:

$$\varepsilon = \frac{\mathrm{Bi}^{-1/2}\alpha^{-1/4}\left[\cosh\left(\mathrm{Bi}^{1/2}\alpha^{-3/4}\right) - 1\right]}{\sinh\left(\mathrm{Bi}^{1/2}\alpha^{-3/4}\right)} \tag{17}$$

This equation is identical to the result obtained by Marchildon and Soliman [6] for the effectiveness of a single detached fin with a rectangular cross-section and a prescribed tip temperature.

Figure 6 shows the effect of Bi on ε at $\beta = 0.2$. The figure shows that ε decreases as Biot number increases. This trend is consistent with the findings of Kundu and Das [10] and Kang [11].

Augmentation factor

The augmentation factor, ψ, is defined as the ratio of the rate of heat transfer transferred to the fluid from the walls and the fins to that which would be transferred from the walls if the fins were not present. The total rate of heat transfer in the presence of the fin is $q_{1\text{-}D}$, and the total rate of heat transfer in the absence of the fin can be expressed:

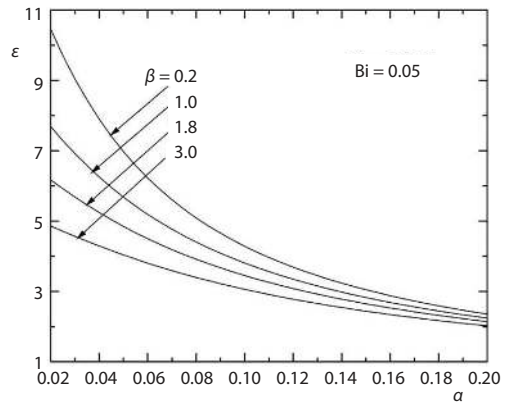

Figure 5. Variation of ε with α and β at Bi = 0.05

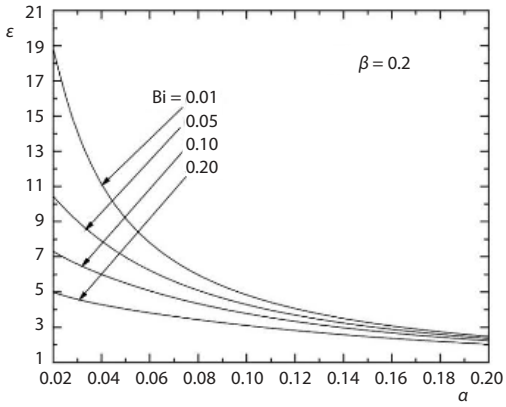

Figure 6. Variation of ε with α and Bi at β = 0.2

$$q_{\mathrm{u}} = \frac{\left(T_1 - T_\infty\right) + \left(T_2 - T_\infty\right)}{\dfrac{W}{kH} + \dfrac{1}{hH}} \tag{18}$$

which can be reduced to the following dimensionless form:

$$Q_{\mathrm{u}} = \frac{q_{\mathrm{u}}}{k\theta_1} = \frac{\gamma\left(1 + \dfrac{\theta_2}{\theta_1}\right)}{\beta + \dfrac{1}{\mathrm{Bi}}} \tag{19}$$

and therefore

$$\psi = \frac{Q_{1\text{-D}}}{Q_{\mathrm{u}}} = 1 + \sqrt{\frac{\sqrt{\alpha}}{\gamma}}\left[\frac{\beta + \dfrac{1}{\mathrm{Bi}}}{\beta + \dfrac{\alpha^{1/4}\mathrm{Bi}^{-1/2}\sinh\left(\mathrm{Bi}^{1/2}\alpha^{-3/4}\right)}{\cosh\left(\mathrm{Bi}^{1/2}\alpha^{-3/4}\right) - 1}} - 1\right] \tag{20}$$

Substituting from eq. (16), eq. (20) simplifies to:

$$\psi = 1 + \frac{\sqrt{\alpha}\left(\varepsilon - 1\right)}{\gamma} \tag{21}$$

Equations (20) and (21) indicate that ψ is dependent on α, β, γ, and Bi, but independent of θ_2/θ_1. For the fixed values Bi = 0.1 and γ = 4, fig. 7 shows the variation of ψ with α and β. These results show that ψ initially increases with α, reaches a maximum, and then decreases with a further increase in α. Since Bi and γ are kept constant, then each constant β curve in fig. 7 corresponds to a fixed value of Q_{u} and the optimum points correspond to maximum $Q_{1\text{-D}}$. It can also be seen that ψ decreases as the wall thickness (indicated by β) increases. As well, the fin aspect ratio corresponding to maximum heat dissipation, $\alpha_{\max}$, increases as the wall thickness increases. This trend is consistent with the findings of Kang [11].

The effects of α and Bi on ψ are demonstrated in fig. 8 for β = 0.2 and γ = 3. Again, since the results correspond to fixed values of β and γ, therefore, each constant Biot number line

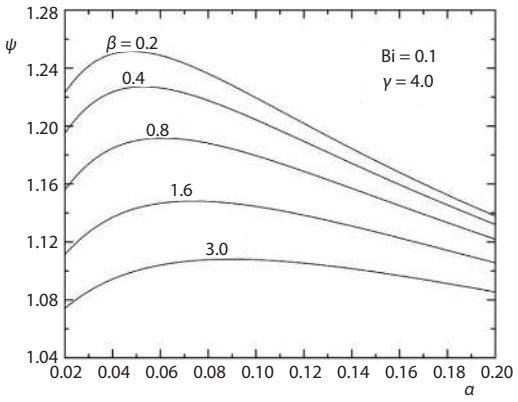

Figure 7. Variation of ψ with α and β for Bi = 0.1 and $\gamma = 4$

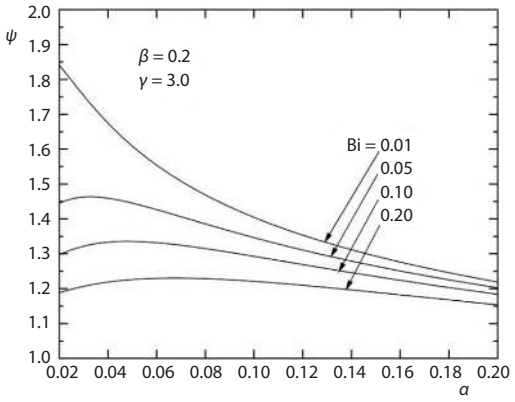

Figure 8. Variation of ψ with α and Bi for $\beta = 0.2$ and $\gamma = 3$

corresponds to a constant value of Q_u and the point where ψ reaches a maximum is also the location of maximum $Q_{1\text{-D}}$. Figure 8 shows that ψ decreases as Biot number increases, consistent with the decrease in ε with the increase in Biot number seen in fig. 6. Also, fig. 8 shows that α_{max} increases as Biot number increases, and for Bi = 0.01, $\beta = 0.2$, and $\gamma = 3$, no optimum was found within the range $0.02 \leq \alpha \leq 0.2$.

Finally, the effect of γ on the parameter ψ is illustrated in fig. 9 for Bi = 0.05. This figure shows that as γ increases, *i.e.*, as the separating distance between the fins increases, ψ decreases since the fin is more effective than the bare wall in dissipating heat. An interesting feature of fig. 9 is that the value of α_{max} does not seem to be affected by the value of γ. Examining eq. (20), we can see that if we equate $\partial\psi/\partial\alpha$ to zero, the parameter γ will cancel out and the value of α_{max} will end up to be a function of β and Biot number only.

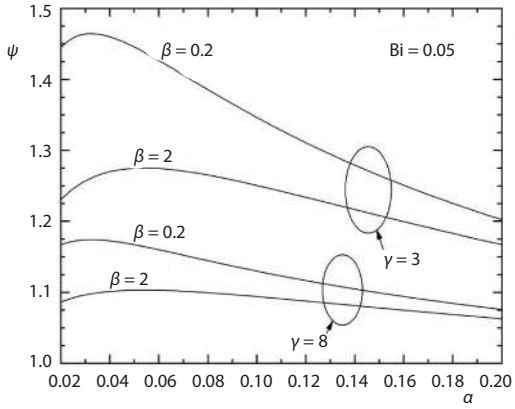

Figure 9. Variation of ψ with β and γ for Bi = 0.05

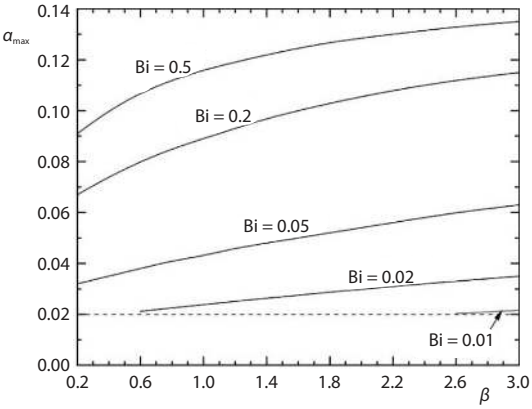

Figure 10. Optimum aspect ratio

It is worthwhile to note that, for the limiting conditions $W = 0$ and $H = t$ (resulting in $\beta = 0$ and $\gamma = \alpha^{1/2}$), the geometry in fig. 1(b) reduces to that of a single detached fin and the physical meaning of ψ reduces to that of ε. Substituting these limiting conditions in eq. (21), the result does confirm the physical expectation.

Optimum dimensions

The results in figs. 7-9 indicate that there is an optimum value of α at which the rate of heat dissipation is maximum and that this optimum aspect ratio is dependent on β and Biot number. The form of this dependence can be determined by differentiating ψ in eq. (20) and equating the result to zero. The resulting expression is shown graphically in fig. 10. As expected, values of α_{max} can be seen to increase as β and/or Biot number increase.

The optimum fin effectiveness, ε_{max}, that corresponds to the optimum aspect ratio was calculated from eq. (17) and the results are shown in fig. 11. Again, ε_{max} can be seen to decrease with an increase in either Biot number or β, consistent with earlier results. Finally, ψ_{max} for the optimum fins is shown in fig. 12 for $\gamma = 3$ and various Biot number, and in fig. 13 for Bi = 0.05 and various γ.

In a typical design procedure, the value of W, see fig.1(b), is selected based on rigidity and stability considerations. In all the results presented previously, the rate of heat transfer from the fin is higher than that from the part of the walls to which the fin is attached (*i.e.*, $\varepsilon > 1$). Therefore, optimizing the total rate of heat transfer, $Q_{1\text{-}D}$, would require a large number of fins with small interfin spacing. This of course would result in excessive pressure drop and poor thermal behavior. Therefore, the interfin spacing is normally determined from manufacturing and thermal-hydraulic considerations. In this study, it will be assumed that both W and H are specified, and the optimum fin that can provide a certain heat duty is to be determined. Figures 10-13 and the corresponding equations can be used in performing this task, as shown in the next example.

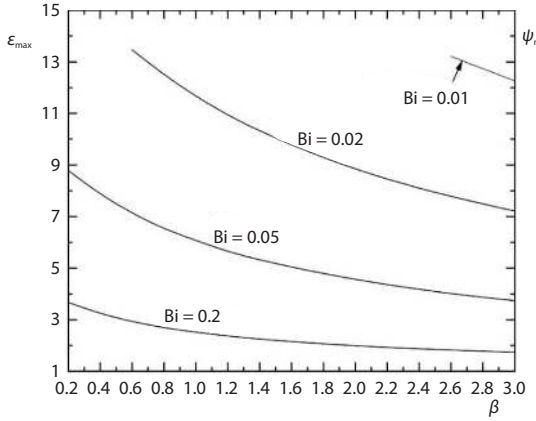

Figure 11. Optimum effectiveness

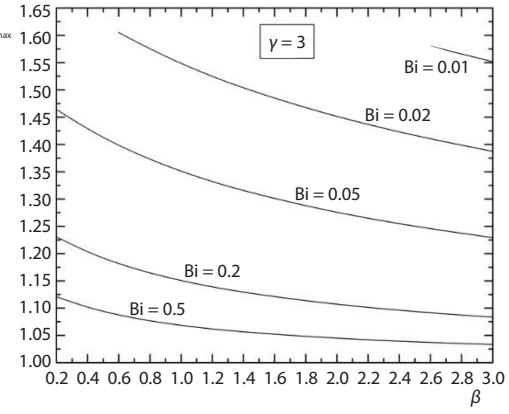

Fig. 12. Optimum augmentation factor for $\gamma = 3$

Example

Consider the geometry in fig. 1(b) with $T_1 = 120$ °C, $T_2 = 70$ °C, $T_\infty = 20$ °C, $k = 50$ W/mK, $h = 100$ W/m^{2}K, $W = 3$ mm, and $H = 10$ cm. It is desired to select optimum fins such that the rate of heat dissipation from the fin and plate surfaces is 30% higher than that of the bare plates.

Solution

The given requirements imply a value of $\psi_{max} = 1.3$. It is now required to determine values of L and t that satisfy this condition. An iterative procedure is required:

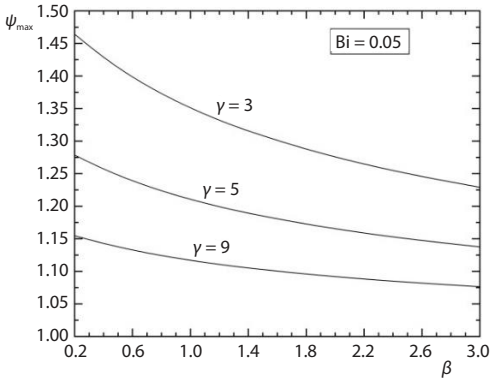

Figure 13. Values of ψ_{max} for Bi = 0.05

– Assume a value for the fin volume per unit depth, Lt.
– Calculate values of Bi, β, and γ using eq. (2).
– Determine α_{max} by formulating the equation $\partial\psi/\partial\alpha = 0$ and doing a root search for the optimum aspect ratio.
– Calculate ε and ψ from eqs. (16) and (20), respectively. Compare this value of ψ with the required value and repeat the aforementioned procedure if the deviation is unacceptable.

This procedure is illustrated in tab. 2.

Table 2. Solution procedure

Iteration No.	Lt [m^{3}m^{-1}]	Bi	β	γ	θ_2/θ_1	α_{max}	$Q_{1\text{-}D}$	Q_u	ψ	ε
0	0.0003	0.0346	0.231	5.77	0.5	0.0263	0.3807	0.2976	1.279	10.94
1	0.0004	0.04	0.2	5	0.5	0.0283	0.3889	0.2976	1.307	10.12
2	0.000375	0.0387	0.207	5.17	0.5	0.0278	0.3871	0.2976	1.300	10.31

Finally, the optimum dimensions are: L_{max} = 11.6 cm and t_{max} = 3.22 cm

Conclusions

The performance of an array of longitudinal rectangular fins attached to two plates at the base and tip (simulating a channel in a plate-fin heat exchanger) was investigated. Dimensionless groups were defined for the geometry and flow parameters. A mesh-independent 2-D solution for the rate of heat transfer was obtained and compared with an approximate 1-D solution. With the value of Biot number limited to Bi ≤ 1, the range of parameters over which the deviation between the two solutions was less than 1% was defined. Results for the fin effectiveness and augmentation factor based on the 1-D solution are presented and discussed and the optimum fin dimensions at which the rate of heat transfer reaches a maximum were obtained. The following conclusions can be made from the present results:

- The fin effectiveness was found to depend significantly on the plate thickness and therefore, results from single-detached fins would be inapplicable. The effectiveness was found to decrease as the plate thickness increased. As well, the effectiveness decreased as the aspect ratio increased, consistent with the behaviour of single detached fins.
- The fin effectiveness was found to decrease as the fin volume increased; a trend that is consistent with earlier findings by Kundu and Das [10] and Kang [11].
- The augmentation factor, ψ, was found to initially increase with the aspect ratio, α, reaches a maximum, and then decreases with a further increase in α. This optimum point corresponds to a maximum rate of heat transfer. The augmentation factor decreased as the wall thickness increased. As well, the fin aspect ratio corresponding to maximum heat dissipation, α_{max}, increased as the wall thickness increased. This trend is consistent with the findings of Kang [11].
- The value of ψ decreased as the fin volume increased, consistent with the decrease in ε with the increase in fin volume. Also, α_{max} increased as the fin volume increased; however, α_{max} was not affected by the inter-fin spacing.

Acknowledgment

The financial assistance provided by the Natural Sciences and Engineering Research Council of Canada (NSERC) under Grant No. RGPIN/409-2013 is gratefully acknowledged.

Nomenclature

Bi – Biot number
H – height of the computational domain, [m]
h – convective heat transfer coefficient, [$Wm^{-2}K^{-1}$]
k – thermal conductivity, [$Wm^{-1}K^{-1}$]
L – fin length, [m]
L_c – characteristic length, [m]
m – fin parameter, [= $(h/kt)^{1/2}$]
N – total number of control volumes
q – rate of heat transfer per unit depth, [Wm^{-1}]
Q – dimensionless rate of heat transfer
T – temperature, [K]
t – fin half thickness, [m]
W – plate thickness, [m]
x, y – co-ordinate system, [m]

Greek symbols

α – aspect ratio
β – dimensionless wall thickness
γ – dimensionless domain height
ε – fin effectiveness
θ – excess temperature, [K]
ψ – augmentation factor

Subscripts

1, 2 – at the outer surfaces of the walls
1-D – 1-D value
2-D – 2-D value
a, b, c, d – components of heat transfer, see fig. 2
max – optimum value
u – without the fin
w – at the contact area between fin and plates
∞ – fluid

References

[1] Kern, D. Q., Kraus, A. D., *Extended Surface Heat Transfer*, McGraw-Hill, New York, USA, 1972
[2] Kraus, A. D., *et al*., *Extended Surface Heat Transfer*, John Wiley and Sons Inc., New York, USA, 2001
[3] Razelos, P., A Critical Review of Extended Heat Transfer, *Heat Transfer Engineering*, *24* (2003), 6, pp. 11-28
[4] Nagarani, N., *et al*., Review of Utilization of Extended Surfaces in Heat Transfer Problems, *Renewable and Sustainable Energy Reviews*, *29* (2014), Jan., pp. 604-613
[5] Soliman, H. M., Elazhary, A., Comment on Cooling Fin Design, *AIAA J. of Thermophysics and Heat Transfer*, *22* (2008), 2, pp. 319-320
[6] Marchildon, A., Soliman, H. M., Optimum Dimensions of Longitudinal Rectangular Fins and Cylindrical Pin Fins with a Prescribed Tip Temperature, *Heat Transfer Engineering*, *40* (2019), 11, pp. 914-923
[7] Alarcon, M., *et al*., Optimisation of a Longitudinal Rectangular Fin-Wall Assembly, *Proceedings*, 12th International Heat Transfer Conference, Grenoble, France, 2002, Vol. 4, pp. 159-164
[8] Kou, H. S., *et al*., Optimum Thermal Analysis of a Heat Sink with Various Cross-Sections by Adjusting Fin Length and Cross-Section, *Heat Transfer Engineering*, 29 (2008), 6, pp. 537-545
[9] Franco, A., An Analytical Method for the Optimum Thermal Design of Longitudinal Fin Arrays, *Heat and Mass Transfer*, *45* (2009), Sept., pp. 1503-1517
[10] Kundu, B., Das, P. K., Performance and Optimum Design Analysis of Convective Fin Arrays Attached to Flat and Curved Primary Surfaces, *International Journal of Refrigeration*, *32* (2009), 3, pp. 430-443
[11] Kang, H. S., Optimization of a Pin Fin with Variable Base Thickness, *ASME Journal of heat Transfer*, *132* (2010), 3, 034501
[12] Lin, S.-J., Chen, Y.-J., Theoretical Determination of Design Parameters for an Arrayed Heat Sink with Vertical Plate Fins, *Heat and Mass Transfer*, *52* (2016), July, pp. 1051-1060
[13] Luna-Abad, J. P., *et al*., The Use of Relative Inverse Thermal Admittance for the Characterization and Optimization of Fin-Wall Assemblies, *Thermal Science*, *21* (2017), 1A, pp. 151-160
[14] Yang, Y., *et al*., Analysis of the Fin Performance of Offset Strip Fins Used in Plate-Fin Heat Exchangers, *ASME Journal of Heat Transfer*, *138* (2016), 10, 101801
[15] Wen, J., *et al.*, Configuration Parameters Design and Optimization for Plate-Fin Heat Exchangers with Serrated Fin by Multi-Objective Genetic Algorithm, *Energy Conversion and Management*, *117* (2016), June, pp. 482-489
[16] Bergman, T. L., *et al*., *Fundamentals of Heat and Mass Transfer*, John Wiley and Sons Inc., New York, USA, 2011

Paper submitted: September 26, 2019
Paper revised: July 29, 2020
Paper accepted: July 31, 2020